Organic & Biomolecular Chemistry

Accepted Manuscript

This article can be cited before page numbers have been issued, to do this please use: V. Kubyshkin and N. Budisa, *Org. Biomol. Chem.*, 2017, DOI: 10.1039/C7OB01421J.

ROYAL SOCIETY OF CHEMISTRY

rsc.li/obc

View Article Online
DOI: 10.1039/C7OB01421J

Organic & Biomolecular Chemistry

ARTICLE

Amide rotation trajectories probed by symmetry

Vladimir Kubyshkin[a]* and Nediljko Budisa[a]*

Received 00th January 20xx,
Accepted 00th January 20xx

DOI: 10.1039/x0xx00000x

www.rsc.org/

The amide rotation of peptidyl-prolyl fragments is an important factor in backbone structure organization of proteins. Computational studies have indicated that this rotation preferentially proceeds through a defined transition-state structure (*syn/exo*). Here, we complement the computational findings by determining the amide bond rotation barriers for the two symmetric proline analogues, *meso* and *racemic* pyrrolidine-2,5-dicarboxylic acid. The rotations around these residues represent *syn/exo* – *syn/exo* and *anti/endo* – *syn/exo* hybrid transition states for the *meso* and *racemic* diastereomer, respectively. The rotation barriers are lower for the former rotation by about 9 kJ mol^{-1} (aqueous medium), suggesting a strong preference for the *syn/exo* (clockwise) rotation over the *anti/endo* (anticlockwise). The results show that both hybrid rotation processes are enthalpically driven but respond differently to solvent polarity changes due to the different transition state dipole-dipole interactions.

Introduction

Proline (**1**, Fig. 1A) plays an important role in various areas of organic and biological chemistry. These include cellular uptake,[1] metabolism,[2] translation,[3] protein folding and engineering,[4] organocatalysis,[5] pre-biotic chemistry,[6] foldamer research,[7] drug design,[8] and more. A particularly interesting focus is the tertiary amide bond formed by peptidyl-prolyl fragments in peptide and protein structures.[9,10] The isomerization of this backbone structure can often become the rate-limiting step in protein folding.[11] This process is frequently facilitated by peptidyl-prolyl *cis-trans* isomerases in natural systems[12] alternatively by substitution of proline with its analogues in laboratory protein expression experiments.[13] Notably, peptidyl-prolyl isomerization is not necessarily slow compared to other amide bond rotations; rather, it may become rate limiting due to the relative thermodynamic stability of the non-native versus the native state.[14]

The two ground states of the *N*-acyl prolyl amide bond are s-*trans* and s-*cis* (Fig. 1B), with *s-trans* conformation forming preferentially. The preference is about 3:1 in Ac-Pro-NHMe,[15] 4:1 in Ac-Pro-OH,[16] 5:1 in Ac-Pro-OMe,[17] and 7:1 in GlyProGly-NH_2[18] and AcGlyGlyProGlyGlyNH$_2$ peptides (water, 298 K),[19] which translates to an approximately 4-5 kJ mol^{-1} in energetic preference. At the same time, the amide bond rotation should proceed through one of the four theoretically possible transition states, in which the amide conjugation should be lost (Fig. 1C). Several structures successfully have depicted the non-conjugated state trapped by a rigid molecular scaffold (so-called twisted amides).[20]

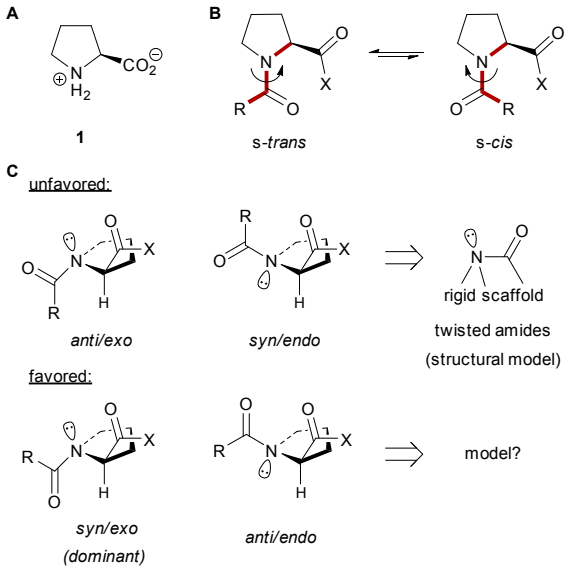

Fig. 1 A. The structure of proline (**1**), B. two *N*-acyl-prolyl ground states, s-*trans* and s-*cis*, C. four possible transition states for the amide rotation, the syn/exo transition state is most favored. The nomenclature is from Ref. 21.

However, these elegant structures do not definitively model the amide transition state due to the following reason. Already in mid 1990s results from a theoretical study showed that the amide rotation preferably proceeds via the *syn/exo* transition states with antiparallel orientation of the N→lone pair and carbonyl C→O dipoles,[21] whereas in the covalent twisted amides this orientation rather resembling parallel. Only very recently metal coordination based twisted amides were reported, and these can model the antiparallel twist.[22]

[a] *Biocatalysis group, Institute of Chemistry, Technical University of Berlin, Müller-Breslau-Str. 10, Berlin 10623, Germany*
E-mails: kubyshkin@win.tu-berlin.de; nediljko.budisa@tu-berlin.de

† Footnotes relating to the title and/or authors should appear here.
Electronic Supplementary Information (ESI) available: Tables S1-S5, copies of the NMR spectra for compounds. See DOI: 10.1039/x0xx00000x

View Article Online
DOI: 10.1039/C7OB01421J

Since the seminal theoretical reports, numerous computational studies have demonstrated that the amide rotation around proline has a preference for the *syn/exo* rotation scenario.[23] These findings are further supported by recent theoretical[24] and experimental[25] studies of the catalytic mechanism of Pin1 peptidyl-prolyl *cis-trans* isomerase, and experimental demonstration of the self-catalytic mechanism of the amide rotation in unpolar media.[26] In the *syn/exo* transition state, the nitrogen lone pair is oriented on the same side and the carbonyl oxygen rotates to the opposite side with respect to the proline carbonyl group, whereas the upstream alkyl moiety is oriented outward. Curiously, despite the existing consensus among theoretical studies, an proper experimental model that addresses the energetic differences in the relevant rotation modes is lacking. While there little doubt that the *syn/exo* transition state is the most relevant, it is not clear whether the *anti/endo* transition state can contribute to the rotation or whether the properties of the *syn/exo* conformation can be extrapolated to other transition scenarios.

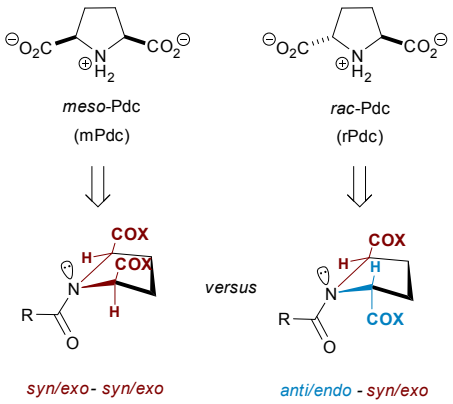

Fig. 2 Design of the study. Two diastereomeric forms of pyrrolidine-2,5-dicarboxylic acid yield different rotation modes around in the *N*-acyl derivatives.

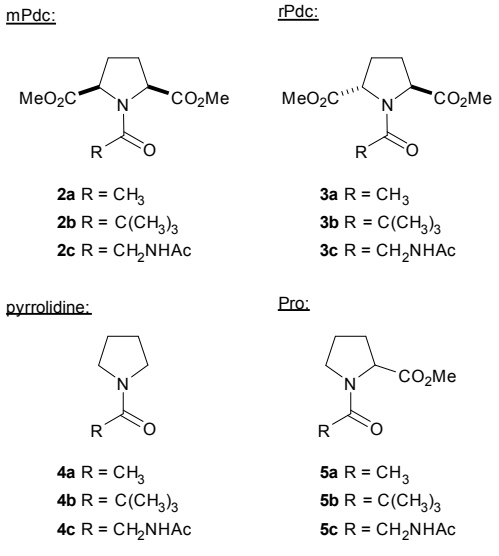

Fig. 3 Examined compounds.

Therefore we designed an experimental model based on derivatives of pyrrolidine-2,5-dicarboxylic acid (Pdc). Pdc has two diastereomeric forms, *meso* (mPdc, with a symmetry plane, σ) and *racemic* (rPdc, with a symmetry axis, C_2). We assumed that the amide ground states are equivalent in the *N*-acyl Pdc derivatives when the acyl-moiety is not chiral. At the same time, we expected the amide rotation to proceed via the *syn/exo* – *syn/exo* hybrid state for mPdc and the *anti/endo* – *syn/exo* hybrid state for rPdc derivatives (Fig. 2) (using the proline transition state nomenclature, Fig 1C). We therefore synthesized a series of amides with non-chiral *N*-terminal acyl groups (Fig. 3). Here, we report the experimental amide bond rotation barriers for these two model situations. The results obtained for proline and pyrrolidine derivatives will also be shown for reference but will not be discussed in the context of the paper.

Results and Discussion

The ground state

We designed our study with the assumption that the amide ground state formed by the Pdc residue will experience similar chemical environments in both diastereomeric situations. The similarity in the through-bond electronic environment of the N-terminal fragment can be assumed from the acidity of the amino acid ammonium salts, which was nearly identical for both Pdc derivatives, as shown in Fig. 4.

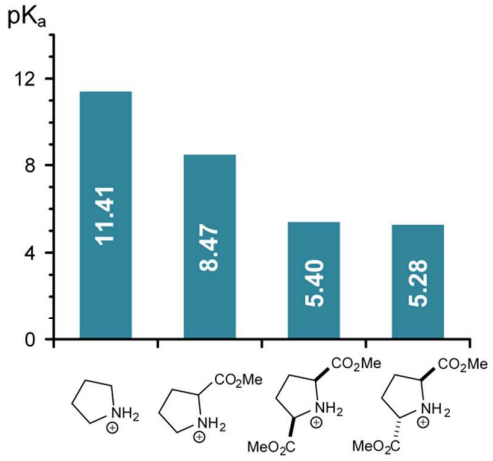

Fig. 4 The pK_a of the ammonium group in the pyrrolidine-2,5-dicarboxylic acid derivatives. The data on pyrrolidine and proline methyl ester are included for comparison. Standard error: ±0.10.

Next, the X-ray crystal structures for both *N*-acetyl derivatives **2a** and **3a** demonstrate fully planar amide bonds (Fig. 5A).[27] In the mPdc derivative **2a**, the amide conformation breaks the symmetry of the structure and creates two enantiomers, which were present at a ratio of 4:2 in the cell unit. In the rPdc derivative **3a**, the amide does not break the existent C_2 symmetry of the structure, and the cell unit contains a racemate with a 2:2 ratio of the (*R,R*) and (*S,S*) enantiomers. The envelope conformation of pyrrolidine ring in

View Article Online
DOI: 10.1039/C7OB01421J

proline is usually described in terms of the *exo-/endo*-pucker nomenclature (alternatively called *up-/down*-) depending on the direction of the C^4-atom displacement from the plane of the ring relative to the carboxyl group orientation. Following this nomenclature, the mPdc derivative **2a** adopts a hybrid of *exo*- and *endo*-pucker, whereas the rPdc derivative **3a** is a hybrid of two *endo*-puckers. The crystal structure is consistent with the solution ^{1}H NMR spectra, in which the two CH(CO_2Me) resonances appear as a triplet and doublet of doublets in **2a** and as two doublets in **3a** (Fig. 5B).[28] Importantly, these NMR spectral signatures persisted in all examined Pdc derivatives and in all employed NMR solvents (see 'Polar effects').

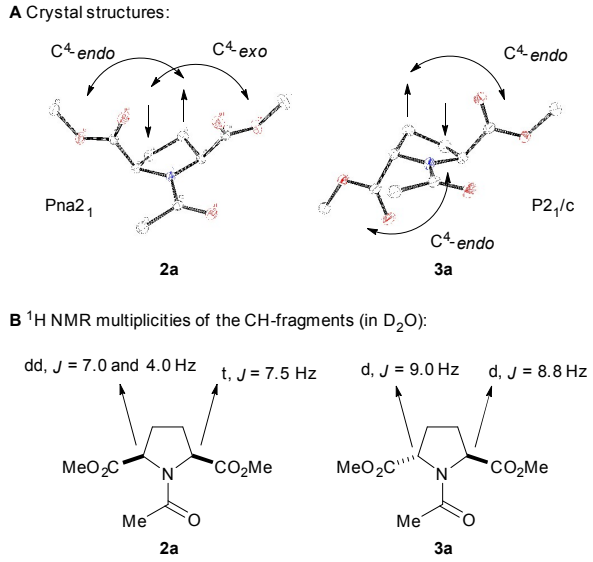

Fig. 5 The X-ray crystal structures (A) and solution ^{1}H NMR (in D_2O) data (B) for the *N*-acetyl compounds **2a** and **3a** are compatible. The ellipsoids represent 30 % probability displacement, carbon – black, oxygen – red, and nitrogen – blue.

Based on this spatial organization argument we expect the steric requirements to be identical around the methyl group of the acetyl moiety, whereas the environment of the carbonyl group is different. These differences are very well described in the proline literature in terms of the pre-organization of the n→π* interaction between the carbonyl groups.[29] As the result, some additional stability of about 1-3 kJ mol^{-1} can be expected for the mPdc derivatives relative to the rPdc-derived compounds.[17]

Another aspect, is the ψ-torsion due to the rotation of the carboxyl-group. For the proline derivative this rotation yields two states ψ_1 ~ 170 and ψ_2 ~ −20° with different polarity. In **5a** the first state is preferred by about 1.3-2.5 kJ mol^{-1}.[30] We modelled the carboxyl-group rotation in **2a**-**3a**, and found that this preference remains nearly identical for the rPdc derivative **3a** ($\Delta\Delta G_{\psi1/\psi2}$ ~ 1.6-2.7 kJ mol^{-1}), whereas in **2a** the two carboxymethyl groups are more proximal, and the rotation state difference becomes more prominent ($\Delta\Delta G_{\psi1/\psi2}$ ~ 3.7-4.7 kJ mol^{-1}). This however, produces only little energy difference between the two ground states, and resulting polarity differences are expected to become influential in unpolar media.[30]

Hereafter, we will not correct for these energies and will consider both ground states equivalent for simplicity of presentation.

Energetic terms of the amide rotation

We then analyzed the amide rotation barriers in the *N*-acetyl derivatives **2a**, **3a** and **4a** in aqueous medium by ^{1}H EXSY NMR. The results are shown on Fig. 6, where the activation energy values $E^{\neq}$ are presented as a function of temperature (also see Tab. S1). As expected, the rotation barrier for the mPdc derivative **2a** was remarkably lower compared to the rPdc derivative **3a** (by 9.3-9.5 kJ mol^{-1}; equivalent to a factor of 43-46 at 298 K).

For all three examined structures, the amide rotation is an enthalpically defined process with a small negative slope $-T\Delta S^{\neq}$ ($\Delta S^{\neq} > 0$). The smallest entropic contribution was found for pyrrolidine derivative **4a** ($\Delta S^{\neq}$ = +3.2±1.8 J mol^{-1} K^{-1}), whereas for the mPdc derivative **2a**, this value was somehow larger ($\Delta S^{\neq}$ = +11.9±0.9 J mol^{-1} K^{-1}). We were not able to determine the entropic value for the rPdc derivative **3a** with the same level of accuracy ($\Delta S^{\neq}$ = +7.6±9.0 J mol^{-1} K^{-1}) due to the high relative experimental error for the very slow rates at the lower temperature conditions. Nonetheless, this lack of accuracy does not affect the overall conclusions, as same tendencies were found for the *N*-acetylglycyl derivatives **2c**-**4c**. In this case, the activation enthalpy was reduced by 5-7 kJ mol^{-1} and the entropy was reduced by 6-9 J mol^{-1} K^{-1} relative to the *N*-acetyl derivatives (See Tab. S2-S3).

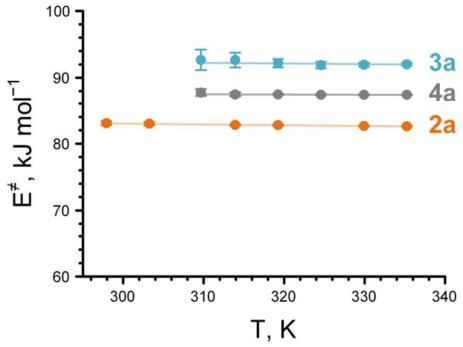

Fig. 6 Amide rotation barriers for the *N*-acetyl derivatives **2a**, **3a** and **4a** as a function of temperature, measured by ^{1}H EXSY NMR in deuterium oxide. For details, see Tab. S1, S3.

A small positive activation entropy is also known for the amide rotation in the proline derivative **5a**, where $\Delta S^{\neq}$ has been reported +9.0 for *cis*→*trans* and +12.8 J mol^{-1} K^{-1} for *trans*→*cis* rotations, respectively.[31,32] The positive entropy of the amide rotation process may originate from the higher molecular rigidity of the ground state (featured by the n→π* interaction, for instance),[15,24] as well as the stronger polar interactions of the ground state with water (organization of the solvent). For example, negative activation entropy for the amide rotation in Ac-AA-OMe has been reported for some

View Article Online
DOI: 10.1039/C7OB01421J

proline analogues with additional polar groups,[33] nonetheless, for some other polar proline analogues this value was also positive.[34]

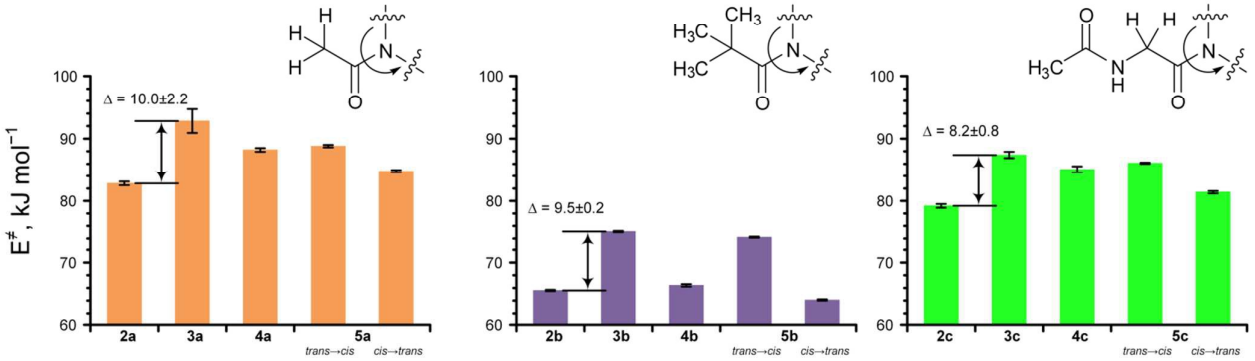

Fig. 7 Amide rotation barriers of the *N*-acyl derivatives. The values were determined in deuterium oxide solution (for AcGly-drrivatives, buffered at pH 7 with potassium phosphate buffer) at 298 or 310 K. See ESI Tab. S4 for details.

Steric bulk of the *N*-acyl substituent

We then measured the amide rotation barriers for the full set of the prepared compounds in deuterium oxide medium (Fig. 7, Tab. S4). The *N*-acetyl (**2a**-**5a**) and *N*-pivaloyl derivatives (**2b**-**5b**) feature the same high symmetry of the acyl moieties, while the steric bulk of the alkyl groups is significantly different. Due to the much higher steric size, the ground state is largely destabilized in the *N*-pivaloyl derivatives, and the overall difference from the *N*-acetyl compounds is about 15-21 kJ mol^{-1} (equivalent to a factor of 500-5000 at 298 K). At the same time, the bulky pivaloyl group excludes the possibility for the *anti/exo* or *syn/endo* transition state situations (proline nomenclature, see Fig. 1C), in which the *tert*-butyl group should move under the pyrrolidine ring. According to our semi-empirical modelling, these will be disfavored by about 11-12 kJ mol^{-1} in both *N*-pivaloyl derivatives **2b**-**3b**, whereas in the *N*-acetyl compounds **2a**-**3a** the disfavor is only by about 4-5 kJ mol^{-1}. Finally, the *N*-acetylglycyl derivatives **2c**-**5c** represent a symmetric *N*-peptidyl-substitution, and the rotation barriers here were reduced by about 3 kJ mol^{-1} (a factor of 3-4 at 298 K) compared to *N*-acetyl compounds **2a**-**5a**. Notably, the amide rotation barriers found for the C-terminal methyl ester derivative of proline **5c** are identical to the found for the C-terminal peptidyl derivative AcGlyGlyProGlyGlyNH$_2$,[19] and from this we may conclude that the C-terminal ester adequately models the amide rotation in the polar medium such as water.

Importantly, for all three types of tested compounds, the rotation barrier difference between the Pdc derivatives was about 8-10 kJ mol^{-1} (a factor of 25-55 at 298 K), with the barriers always lower for the mPdc derivative. This result confirms that the rotation barrier difference in this case originates from the transition state structures. In both the *syn/exo* and *anti/endo* transition states shown in Fig 1C, the alkyl group of the acetyl moiety moves outwards and cannot sterically interfere with the substituents in the pyrrolidine ring (see also Fig. 2). On the other hand, the carbonyl group of the amide fragment moves towards the pyrrolidine ring and may sterically interfere with a carboxymethyl group in rPdc derivatives and create polar interactions with the carboxymethyl groups in both rPdc and mPdc derivatives.

Polar effects

The polar interactions between the amide and carboxymethyl groups were then studied by comparison of the rotation barriers of the *N*-acetyl compounds (**2a**, **3a**, **4a**) in a set of nine NMR solvents (see Tab. S5). It is well known that the conjugation in the amide ground state is highly dependent on the solvent polarity;[9,35] mechanistically, this is illustrated by the change in the amide resonance contributions [O=C-N ↔ $^{-}$O-C=N^{+}]. The Reichardt-Dimroth parameter (E_T) is a solvatochromic value that quantifies the ability of a solvent to separate intramolecular charges. Therefore, plotting rotation barriers in the $E^{\neq} - E_T$ coordinates produces positive slopes due to the differences in the ground state stabilities.[16]

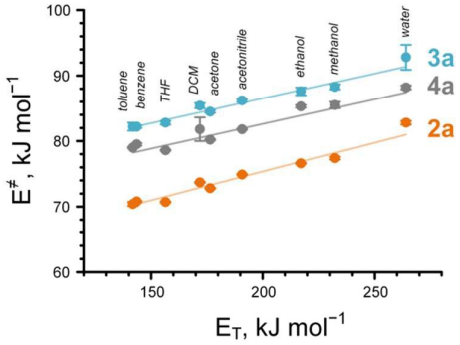

Fig. 8 Amide rotation barriers for the *N*-acetyl derivatives **2a**, **3a** and **4a** measured in different solvents by ^{1}H EXSY NMR (at 298 or 310 K). For details see ESI Tab. S4.

View Article Online
DOI: 10.1039/C7OB01421J

While the experimental slopes (Fig. 8) for the rPdc and pyrrolidine derivatives (**3a** and **4a**) were nearly identical (0.076±0.006 and 0.075±0.010, respectively), the slope for the mPdc derivative (**2a**) was notably larger (0.088±0.008). This result illustrates differences in the polar effects of the transition states. We performed semi-empirical modelling of the amide rotation, and found that the overall molecular dipole follows the orientation of the amide carbonyl group C=O in the pyrrolidine derivative **4a**, as well as in the rPdc derivative **3a**. In the latter compound the dipolar contribution of both carboxymethyl-moieties is mutually compensated by the C_2-symmetry of the residue (Fig. 9). As the result, the overall molecular dipole is defined by the orientation of the amide carbonyl group, and effectively, both **3a** and **4a** yield the same slope in the $E^{\neq} - E_T$ coordinates.

The orientation of the molecular dipole in **2a** is more complex. The configuration of the two carboxymethyl substituents renders the compound more polar than **3a**. For example, the R_f of mPdc derivatives are consistently lower compared with the equivalent rPdc derivatives (see Experimental section). Higher polarity of the *meso*-diastereomer is also inferred from the octan-1-ol/water partitioning values as shown on Fig. 9. The amide rotation via the putative *syn/exo* – *syn/exo* hybrid transition state partially compensates for the intramolecular dipole-dipole in the transition state, causing the transition state to be relatively favored in the nonpolar solvents. As the result, the slope in the $E^{\neq} - E_T$ coordinates increases. Similar dipolar compensation can be expected for the amide rotation via the *syn/exo* transition state in peptidyl-prolyl fragments, and this effect might be enhanced due to a higher polarity of the amide fragment versus the esters reported here. As a result, the *syn/exo* transition state dominance should increase in less polar environments.

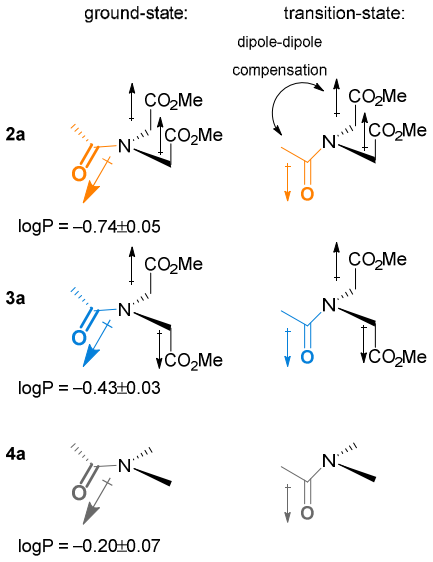

Fig. 9 Schematic representation of the dipolar effects during the amide rotation in *N*-acetylated compounds. LogP values represent partitioning of the compounds between octan-1-ol and water at 298 K.

Conclusions

In summary, we described the amide rotation properties in *N*-acyl pyrrolidine-2,5-dicarboxylic acid derivatives, capped at the C-terminal sides as methyl esters. The *meso* diastereomer of this compound exhibited an amide rotation barrier of approximately 9 kJ mol^{-1} lower than that of the *racemic* diastereomer. This outcome was reproducible in three *N*-acyl derivatives with different degrees of steric bulk of the acyl-moieties to represent varying ground state energies.

This model system allowed us to demonstrate experimental features of the amide rotation relevant for peptidyl-prolyl groups: 1) the transitions are enthalpically driven and 2) differ in dipole-dipole compensation levels in the transition states and 3) *syn/exo* transition scheme prevails in general over the *anti/endo*. These conclusions are consistent with the results of computational studies, which suggested dominance of the *syn/exo* over the *anti/endo* transition state. At the same time, the other theoretically possible transition states, *anti/exo* and especially *syn/endo*, are expected to be disfavoured in peptide structures, as these would require movement of a bulky upstream peptidyl-fragment under the pyrrolidine ring of proline.

Experimental section

Synthesis

The *N*-benzyl derivatives of Pdc were prepared starting from adipic acid as a mixture of two diastereomers.[36] The resulting Bn-(MeO)Pdc-OMe compounds were separated on a silica gel column using hexane – ethyl acetate (4:1) as an eluent (R_f = 0.48 for rPdc and 0.27 for mPdc derivative). The ^{1}H NMR spectra exhibit a characteristic AB system for the diastereotopic benzyl CH_2 group in the rPdc derivative, whereas this signal is a singlet in the mPdc derivative, where the CH_2 moiety is not diastereotopic. ^{1}H NMR (500 MHz, $CDCl_3$), δ: Bn-(MeO)mPdc-OMe, 7.44-7.32 (m, 5H), 4.05 (s, 2H), 3.68 (s, 6H), 3.59 (br, 2H), 2.18 (m, 4H); Bn-(MeO)rPdc-OMe, 7.44-7.32 (m, 5H), 4.11 (d, *J* = 13 Hz, 1H), 3.92 (br d, *J* = 7 Hz, 2H), 3.91 (d, *J* = 13 Hz, 1H), 3.75 (s, 6H), 2.42 (m, 2H), 2.04 (m, 2H). The removal of the *N*-benzyl group was performed by stirring of the substance with palladium on charcoal (10%) in methanol acidified with an equivalent amount of hydrochloric acid, under hydrogen pressure (40 atm), at 35 °C. The reaction was monitored by NMR. After the reaction was complete, the mixture was filtered, the solvent was removed under reduced pressure, and the residue was dissolved in water, filtered with activated charcoal and freeze-dried. The amino acid hydrochlorides were obtained as pinkish powders. ^{1}H NMR (700 MHz, CD_3OD), δ: HCl·H-(MeO)mPdc-OMe, 4.33 (t, *J* = 6 Hz, 2H), 3.85 (s, 6H), 2.40 (m, 2H), 2.15 (m, 2H); HCl·H-(MeO)rPdc-OMe, 4.22 (t, *J* = 6 Hz, 2H), 3.80 (s, 6H), 2.32 (m, 2H), 2.06 (m, 2H).

View Article Online
DOI: 10.1039/C7OB01421J

***N*-acetyl compounds** were prepared as follows. A salt HCl·H-(MeO)Pdc-OMe (Pdc = mPdc or rPdc, 101 mg, 0.45 mmol) was stirred with acetic anhydride (0.4 ml, 4.2 mmol, 9 equiv.), triethylamine (0.2 ml, 1.4 mmol, 3 equiv.) and dimethylaminopyridine (5 mg, 0.04 mmol, 9 mol %) in a dichloromethane – tetrahydrofuran mixture (1.5 ml, 2:1) for 48 hours at room temperature. The solvent was gently removed under nitrogen gas flow, and the residue was dissolved in water (0.7 ml) and freeze-dried. The crude material was purified on a short silica gel column (about 10 g) using an ethyl acetate – methanol mixture (19:1) as an eluent (R_f = 0.49 for **2a** and 0.63 for **3a**).

Dimethyl (*r,s*)-1-acetylpyrrolidine-2,5-dicarboxylate (**2a**). Yellowish solid, yield 84 mg (0.37 mmol, 81 %). ^{1}H NMR (700 MHz, D_2O), δ: 4.74 (dd, *J* = 7.0, 4.0 Hz, 1H), 4.44 (t, *J* = 7.5 Hz, 1H), 3.75 (s, 3H), 3.69 (s, 3H), 2.33-2.26 (m, 3H), 2.03 (s, 3H), 1.92 (m, 1H). ^{13}C{^{1}H} NMR (176 MHz, D_2O), δ (all singlets): 173.9 (C=O), 173.8 (C=O), 173.3 (C=O), 61.2 (CH), 60.1 (CH), 53.1 (CH_3O), 52.8 (CH_3O), 29.4 (s, CH_2), 27.7 (CH_2), 21.2 (CH_3). HMRS (ESI-orbitrap): calcd. for $[M+H]^+$ $C_{10}H_{16}NO_5$ 230.1023 Da, found 230.1028 Th. M.p. 60-65 °C.

Dimethyl (*r,r*)-1-acetylpyrrolidine-2,5-dicarboxylate (**3a**). White solid, yield 85 mg (0.37 mmol, 82 %). ^{1}H NMR (700 MHz, D_2O), δ: 4.82 (d, *J* = 9.0 Hz, 1H), 4.54 (t, *J* = 8.8 Hz, 1H), 3.75 (s, 3H), 3.69 (s, 3H), 2.36 (m, 1H), 2.22 (m, 2H), 2.05 (m, 1H), 2.00 (s, 3H). ^{13}C{^{1}H} NMR (176 MHz, D_2O), δ (all singlets): 174.2 (C=O), 174.0 (C=O), 173.7 (C=O), 61.1 (CH), 59.5 (CH), 53.4 (CH_3O), 53.0 (CH_3O), 29.2 (s, CH_2), 27.0 (CH_2), 21.1 (CH_3). HMRS (ESI-orbitrap): calcd. for $[M+H]^+$ $C_{10}H_{16}NO_5$ 230.1023 Da, found 230.1030 Th. M.p. 95-100 °C.

The proline derivative Ac-Pro-OMe (**5a**) was prepared by mixing commercial racemic HCl·Pro-OMe with an equivalent amount of acetic anhydride in dichloromethane solution. Solvent was removed under reduced pressure, and the crude material was purified using a hexane – ethyl acetate gradient elution (from 1:1 to 0:1). The substance was obtained as a clear oil, which crystallized upon long time storage at 4 °C. White solid, m.p. 35-40 °C. ^{1}H NMR (700 MHz, D_2O), δ (two rotamers, $K_{trans/cis}$ 4.95±0.05 at 298 K): 4.62 (s-*cis*, dd, *J* = 8.8, 2.6 Hz) and 4.36 (s-*trans*, dd, *J* = 8.8, 4.6 Hz, 1H, α-CH), 3.72 (s-*cis*, s) and 3.67 (s, s-*trans*, 3H, CH_3O), 3.59 and 3.55 (s-*trans*, two m) and 3.46 and 3.39 (s-*cis*, two m, 2H, δ-CH_2), 2.28 and 2.15 (s-*cis*, two m) and 2.23 and 1.94 (s-*trans*, two m, 2H, β-CH_2), 2.05 (s-*trans*, s) and 1.93 (s-*cis*, s, 3H, CH_3C=O), 1.95 (s-*trans*, m) and 1.90 and 1.80 (s-*cis*, two m, 2H, γ-CH_2).

N-acetyl pyrrolidine **4a** was prepared as follows. Pyrrolidine (0.25 ml, 3 mmol) was mixed with acetic anhydride (0.29 ml, 3 mmol, 1 equiv.) in dichloromethane (5 ml) (*CAUTION:* vigorous reaction!). The mixture was stirred at room temperature for 30 min. Sodium carbonate (0.3 g) was added, and this mixture was shaken for about 15 hours at room temperature. The mixture was filtered, and the solvent was removed under reduced pressure to give **4a** as a clear liquid. Yield 0.26 g (2.3 mmol, 75 %). ^{1}H NMR (500 MHz, D_2O), δ: 3.41 (t, *J* = 7.0 Hz, 2H), 3.28 (t, *J* = 7.0 Hz, 2H), 1.97 (s, 3H), 1.86 (m, 2H), 1.79 (m, 2H).

***N*-pivaloyl compounds** were prepared according to the procedure for **5b** synthesis.[37] A salt HCl·H-(MeO)Pdc-OMe (Pdc = mPdc or rPdc, 101 mg, 0.45 mmol) was mixed with pivaloyl chloride (70 µl, 0.57 mmol, 1.3 equiv.) in dichloromethane (1.5 ml), followed by addition of triethylamine (150 µl, 1.08 mmol, 2.4 equiv.) and dimethylaminopyridine (5 mg, 0.04 mmol, 9 mol %). The mixture was stirred at room temperature for 4 hours. Then, it was washed with water (1x0.3 ml), 1 M aqueous hydrochloric acid (1x0.3 ml) and 1 M sodium hydrogencarbonate solution (1x0.3 ml), and subsequently dried over sodium sulphate, filtered and evaporated. Crude material was purified on a silica gel column (about 5 g), using a hexane – ethyl acetate mixture (1:1) as an eluent (R_f= 0.41 for **2b** and 0.51 for **3b**).

Dimethyl (*r,s*)-1-pivaloylpyrrolidine-2,5-dicarboxylate (**2b**). Clear oil, yield 80 mg (0.29 mmol, 66 %). ^{1}H NMR (700 MHz, D_2O), δ: 5.03 (br d, *J* = 7 Hz, 1H), 4.43 (br t, *J* = 8 Hz, 1H), 3.72 (br s, 3H), 3.69 (br s, 3H), 2.26 (br m, 3H), 1.77 (br m, 1H), 1.13 (s, 9H). ^{13}C{^{1}H} NMR (176 MHz, D_2O), δ (all singlets): 180.7 (C=O), 174.3 (C=O), 174.0 (C=O), 62.8 (CH), 60.8 (CH), 53.0 (CH_3O), 52.6 (CH_3O), 39.2 (C), 31.1 (CH_2), 26.7 (CH_3), 25.4 (CH_2). HMRS (ESI-orbitrap): calcd. for $[M+1]^+$ $C_{13}H_{22}NO_5$ 272.1492 Da, found 272.1492 Th.

Dimethyl (*r,r*)-1-pivaloylpyrrolidine-2,5-dicarboxylate (**3b**). White solid, yield 86 mg (0.32 mmol, 70 %). ^{1}H NMR (700 MHz, D_2O), δ: 5.14 (d, *J* = 8.5 Hz, 1H), 4.52 (d, *J* = 9.8 Hz, 1H), 3.74 (s, 3H), 3.67 (s, 3H), 2.38 (m, 1H), 2.19 (dd, *J* = 13.2, 6.6 Hz, 1H), 2.09 (m, 1H), 1.92 (dd, *J* = 13.5, 7.2 Hz, 1H), 1.12 (s, 9H). ^{13}C{^{1}H} NMR (176 MHz, D_2O), δ (all singlets): 180.4 (C=O), 175.1 (C=O), 174.8 (C=O), 61.9 (CH), 60.9 (CH), 53.4 (CH_3O), 52.8 (CH_3O), 39.1 (C), 30.3 (CH_2), 26.5 (CH_3), 24.8 (CH_2). HMRS (ESI-orbitrap): calcd. for $[M+1]^+$ $C_{13}H_{22}NO_5$ 272.1492 Da, found 272.1494 Th. M.p. 80-85 °C.

The synthesis of **5b** was fully reproduced[37] starting from 0.5 g of the racemic HCl·H-Pro-OMe (3.0 mmol, 1/10 scale of the reported synthesis). The product was a colorless oil. Yield 0.60 g (2.8 mmol, 92 %). ^{1}H NMR (700 MHz, D_2O), δ (s-*trans* rotamer only, $K_{trans/cis}$ = 46±2 at 298 K): 4.34 (dd, *J* = 8.5, 6.0 Hz, 1H, α-CH), 3.79 (dt, *J* = 10.6, 6.5 Hz, 1H, δ-CH), 3.74 (dt, *J* = 10.6, 6.7 Hz, 1H, δ-CH), 3.67 (s, 3H, CH_3O), 2.14 (m, 1H, β-CH), 1.98 (m, 1H, γ-CH), 1.92 (m, 1H, γ-CH), 1.79 (m, 1H, β-CH), 1.17 (s, 9H, $(CH_3)_3C$).

Compound **4b** was prepared as follows. Pyrrolidine (1 ml, 12.2 mmol) was mixed with triethylamine (3.4 ml, 24.4 mmol, 2 equiv.) in dichloromethane (20 ml). Pivaloyl chloride (1.6 ml, 13.0 mmol, 1.07 equiv.) was added dropwise at the room temperature (*CAUTION:* vigorous reaction!), and the mixture was stirred for an additional 30 min. The solution was washed with water (1x5 ml), 1:2 aqueous hydrochloric acid (1x5 ml) and 1 M sodium hydrogen carbonate (1x5 ml); subsequently, it was dried over sodium sulphate, filtered and evaporated. Pure **4b** was obtained as a colorless solid after crystallization from dichloromethane. Yield 1.80 g (11.6 mmol, 95 %). ^{1}H NMR (700 MHz, D_2O), δ: 3.62 (t, *J* = 6.1 Hz, 2H), 3.34 (t, *J* = 6.7 Hz, 2H), 1.86 (m, 2H), 1.73 (m, 2H), 1.16 (s, 9H). M. p. 57-63 °C.

***N*-acetylglycyl (*N*-aceturyl) compounds** were prepared by using solution peptide coupling conditions. Aceturic acid (78

View Article Online
DOI: 10.1039/C7OB01421J

mg, 0.67 mmol, 1.3 equiv.) was mixed with benzotriazol-1-yl-oxytripyrrolidinophosphonium hexafluorophosphate (PyBOP, 346 mg, 0.66 mmol, 1.3 equiv.) and diisopropylethylamine (120 µl, 0.69 mmol, 1.35 equiv.) in dichloromethane (2 ml). After about 10 min, the resulting solution was added to the mixture of HCl·H-(MeO)Pdc-OMe (Pdc = mPdc or rPdc, 113 mg, 0.51 mmol) with diisopropylethylamine (220 µl, 1.26 mmol, 2.5 equiv.) in dichloromethane (4 ml). The mixture was stirred for about 10 hours. It was then washed with 1:2 aqueous hydrochloric acid (1x0.5 ml) and 1 M sodium hydrogen carbonate (1x0.5 ml); subsequently, it was dried over sodium sulphate, filtered and evaporated. The resulting oil was extracted with water (1.5 ml). The extract was filtered through a short cation-exchange column (1.5 ml), and elution was performed with water (about 5 ml). The aqueous fractions were collected and freeze-dried. Final purification was afforded by silica gel chromatography (about 10 g) using an ethyl acetate – methanol gradient elution (19:1 – 4:1 – 0:1). The resulting compounds were colorless glassy materials and were slightly acidic. Therefore, the NMR samples in deuterium oxide were buffered with potassium phosphate buffer (70 mM, pH 7) and contained 35 mM of the analytes.

Dimethyl (*r,s*)-1-(acetylglycyl)pyrrolidine-2,5-dicarboxylate (**2c**). Yield 34 mg (0.12 mmol, 24 %). ^{1}H NMR (700 MHz, D_2O), δ: 4.78 (dd, *J* = 7.9, 2.0 Hz, 1H), 4.47 (t, *J* = 7.8 Hz, 1H), 4.08 (d, *J* = 17.3 Hz, 1H), 3.93 (d, *J* = 17.1 Hz, 1H), 3.75 (s, 3H), 3. 68 (s, 3H), 2.34-2.24 (m, 3H), 1.98 (s, 3H), 1.89 (m, 1H). ^{13}C{^{1}H} NMR (176 MHz, D_2O), δ (all singlets): 174.6 (C=O), 173.8 (C=O), 172.8 (C=O), 170.5 (C=O), 60.6 (CH), 59.9 (CH), 53.2 (CH_3O), 52.9 (CH_3O), 41.5 (NH-CH_2), 29.4 (CH_2), 27.2 (CH_2), 21.6 (CH_3). HRMS (ESI-orbitrap): calcd. for $[M+H]^+$ $C_{12}H_{19}N_2O_6$ 287.1238 Da, found 230.1240 Th.

Dimethyl (*r,r*)-1-(acetylglycyl)pyrrolidine-2,5-dicarboxylate (**3c**). Yield 37 mg (0.13 mmol, 26 %). ^{1}H NMR (700 MHz, D_2O), δ: 4.85 (d, *J* = 8.8 Hz, 1H), 4.56 (d, *J* = 9.4 Hz, 1H), 4.03 (d, *J* = 17.3 Hz, 1H), 3.84 (d, *J* = 17.3 Hz, 1H), 3.75 (s, 3H), 3.69 (s, 3H), 2.36 (m, 1H), 2.26 (dd, *J* = 13.6, 6.8 Hz, 1H), 2.17 (m, 1H), 2.04 (dd, *J* = 13.5, 7.0 Hz, 1H), 1.97 (s, 3H). ^{13}C{^{1}H} NMR (176 MHz, D_2O), δ (all singlets): 174.5 (C=O), 174.0 (C=O), 173.5 (C=O), 170.4 (C=O), 60.0 (CH), 59.7 (CH), 53.5 (CH_3O), 53.0 (CH_3O), 41.5 (NH-CH_2), 29.3 (CH_2), 26.4 (CH_2), 21.5 (CH_3). HRMS (ESI-orbitrap): calcd. for $[M+H]^+$ $C_{12}H_{19}N_2O_6$ 287.1238 Da, found 230.1239 Th.

The other two peptides **4c** and **5c** were prepared using analogous conditions, by employing *N*,*N*,*N*',*N*'-tetramethyl-*O*-(*N*-succinimidyl)uronium hexafluorophosphate (HSTU) as the coupling reagent. **4c**, ^{1}H NMR (700 MHz, D_2O), δ: 3.93 (s, 2H), 3.40 (t, *J* = 6.9 Hz, 2H), 3.33 (t, *J* = 6.9 Hz, 2H), 1.98 (s, 3H), 1.90 (m, 2H), 1.80 (m, 2H). HRMS (ESI-orbitrap): calcd. for $[M+H]^+$ $C_8H_{15}N_2O_2$ 171.1128 Da, found 171.1129 Th. **5c**, ^{1}H NMR (700 MHz, D_2O), δ (s-*trans* rotamer only, $K_{trans/cis}$ = 6.15±0.27 at 298 K): 4.41 (dd, *J* = 9.0, 4.4 Hz, 1H, α-CH), 4.03 (d, *J* = 17.3 Hz, 1H), 3.98 (d, *J* = 17.5 Hz, 1H), 3.68 (s, 3H, CH_3O), 3.58 (m, 1H, δ-CH), 3.54 (m, 1H, δ-CH), 2.22 (m, 1H, β-CH), 1.98 (s, 3H), 1.97 (m, 2H, γ-CH_2), 1.96 (m, 1H, β-CH). HRMS (ESI-orbitrap): calcd. for $[M+H]^+$ $C_{10}H_{17}N_2O_4$ 229.1183 Da, found 229.1182 Th.

Physical chemistry

The NMR measurements were performed by 700 and 500 MHz ^{1}H NMR detection. The variable temperature unit was calibrated using acidified methanol sample measurements.[38]

The pK_a measurements were performed at 298 K as described.[16] Buffer samples were taken at different pH values. Deuterium oxide was added (1/10 to the buffer volume), and the analyte (pyrrolidine or methyl ester hydrochlorides of the amino acids) solution in a little amount of deuterium oxide was added 1-2 min prior to the ^{1}H NMR measurement. The ^{1}H NMR spectra were recorded using a W5 water suppression pulse tray. The final analyte concentration was 0.5-1 mM. The measurements were performed in 10 mM phosphate buffer for pyrrolidine, 50 mM/60 mM phosphate/glycine buffer for HCl·H-Pro-OMe, and 20 mM/3 mM phosphate/citric buffer for HCl·H-(MeO)Pdc-OMe analytes. The standard error of the measured pK_a values is ±0.10. For pyrrolidine the obtained value 11.41 is consistent with the previously reported 11.35.[39]

Partitioning was measured as follows. 5 mg of a compound was shaken with octan-1-ol (1.00 ml) and deionized water (1.00 ml) at 298±2 K for 24 hours. Aliquotes (250 µl) were taken to same type NMR tubes and diluted with acetonitrile-d_3 (200 µl) for locking and shimming. The concentration of the samples were measured in single scan 90-degree pulse ^{1}H NMR spectra recorded at 298 K. Only the 90-degree pulses and zero-phase values were re-adjusted between the measurements. The method is similar to the recently reported by Linclau et al. based on ^{19}F NMR detection.[40] Found logP values: **2a** −0.74±0.05, **3a** −0.43±0.03, **4a** −0.20±0.07, **5a** −0.44±0.05.

The amide rotation kinetics were measured in ^{1}H cross-relaxation experiments (NOESY/EXSY with z-gradients) as described.[16,19] The analyte concentration in the NMR samples was 30-80 mM. Between 2-5 different mixing times (15 ms – 5 s) were used for the exchange detection. The time domain in the direct dimension was 2048 points, whereas in the indirect dimension, this was inset to yield sufficient resolution of the analysed resonances (160-512 points, resolution 5-30 Hz). Recycling delay was ≥2·T_1 of the analysed resonances. Note that the use of a high recycling delay is not necessary but improves the precision of the measurements. The exchange rate matrices were calculated using EXSYCalc (Mestrec), and the kinetic constants were converted to the activation energy values using the Eyring equation. The error of the activation energy values was calculated using the rate constant error and does not take into account the temperature calibration error. The results are summarized in ESI in Tab. S1 ($E^{\neq}$ for **2a**-**4a** at different temperatures), Tab. S2 ($E^{\neq}$ for **2c**-**4c** at different temperatures), S3 (energetic terms for **2a**-**4a** and **2c**-**4c**), S4 ($E^{\neq}$ in all compounds, D_2O), S5 ($E^{\neq}$ for **2a**-**4a** in different solvents).

Molecular modelling was performed in Scigress Modelling 3.2 (Fujitsu, Poland). PM6-water algorithm was used for semi-empirical calculations, and B88-PW91 GGA functional was employed for the DFT optimizations.

View Article Online
DOI: 10.1039/C7OB01421J

X-ray diffraction measurements were performed at 150 K. The R-factor for the calculated structures was 0.0257 (**2a**) and 0.0346 (**3a**).

Acknowledgements

VK acknowledges DFG research group 1805 for a postdoctoral position and Synpeptide EU consortium for financial support. The authors are also grateful to Dr Marcie Jaffee (Atlanta, USA) for generous proof-reading of the manuscript.

The article is dedicated to the memory of Prof Yuriy Kholin (1962-2017), who nurtured a generation of young talented Ukrainian chemists.

Conflict of Interest

There is no conflict of interest to declare to this article.

Notes and references

[1] Proline/sodium symport is utilized by some organisms for the uptake of proline as a nutrient: a) C.-C. Chen, T. Tsuchiya, Y. Yamane, J. M. Wood and T. H. Wilson, *J. Membr. Biol.*, 1985, **84**, 157-164; b) S. Moses, T. Sinner, A. Zaprasis, N. Stöveken, T. Hoffman, B. R. Belitsky, A. L. Sonenshein and E. Bremen, *J. Bacteriol.*, 2012, **194**, 745-758; c) H. Jung, D. Hilger and M. Raba, *Front. Biosci.*, 2012, **1**, 745-759.

[2] a) L. Szabados and A. Savouré, *Trends Plant. Sci.*, 2010, **15**, 89-97; b) I. Pérez-Arellano, F. Carmona-Álvarez, A. I. Martínez, J. Rodríguez-Díaz, J. Cervera, *Protein Sci.*, 2010, **19**, 372-382.

[3] The ribosomal peptide bond formation for proline is slow compared to other amino acids: a) M. Y. Pavlov, R. E. Watts, Z. Tan, V. W. Cornish, M. Ehrenberg and A. C. Forster, *Proc. Natl. Acad. Sci. USA*, 2009, **106**, 50-54; b) L. K. Doerfel, I. Wohlgemuth, C. Kothe, F. Peske, H. Ulraub and M. V. Rodnina, *Science*, 2013, **339**, 85–88; c) L. K. Doerfel, I. Wohlgemuth, V. Kubyshkin, A. L. Starosta, D. N. Wilson, N. Budisa and M. V. Rodnina, *J. Am. Chem. Soc.*, 2015, **137**, 12997–13006.

[4] a) A. Farhat-Khemakhem, M. B. Ali, I. Boukhris, B. Khemachem, E. Maguin, S. Bejar and H. Chouayekh, *Int. J. Biol. Macromol.*, 2013, **54**, 9-15; b) J. Huang, B. J. Jones and R. J. Kazlauskas, *Biochemistry*, 2015, **54**, 4330-4341; c) H. Yu, Y. Zhao, C. Guo, Y. Gan and H. Huang, *Biochim. Biophys. Acta – Prot. Proteom.*, 2015, **1854**, 65-72.

[5] Proline and its derivatives catalyse condensation reactions either as an organic additive: a) S. Bertelsen and K. A. Jørgensen, *Chem. Soc. Rev.*, 2009, **38**, 2178-2189; or this could also be an *N*-terminal proline residue in a short peptide: b) J. Duschmalé, J. Wiest, M. Wiesner and H. Wennemers, *Chem. Sci.*, 2013, **4**, 1312-1318; c) T. Schnitzer, M. Wiesner, P. Krattiger, J. D. Revell and H. Wennemers, *Org. Biomol. Chem.*, 2017, DOI: 10.1039/C7OB01039G; or a protein: c) M. Rahimi, E. M. Geertsema, Y. Miao, J.-Y. van der Meer, T. van den Bosch, P. de Haan, E. Zandvoort and G. J. Poelarends, *Org. Biomol. Chem.*, 2017, **15**, 2809-2816.

[6] Studies suggest a role of proline in the homochirality transfer from amino acids to sugars: J. E. Hein and D. G. Blackmond, *Acc. Chem. Res.*, 2012, **45**, 2045-2054.

[7] a) S. Kheria, R. V. Nair, A. S. Kotmale, P. R. Rajamohanan and G. J. Sanjayan, *New. J. Chem.*, 2015, **39**, 3327-3332; b) N. D. Bansode, M. V. Sonar and K. N. Ganesh, *Chem. Commun.*, 2016, **52**, 4884-4887.

[8] I. E. Sampaio-Dias, C. A. D. Sousa, X. Garcia-Mera, J. F. da Costa, O. Caamaño and J. E. Rodriguez-Borges, *Org. Biomol. Chem.*, 2016, **14**, 11065-11069.

[9] *cis-trans-Isomerization in Biochemistry*, ed. C. Dugave, Wiley, Weinheim, 2006.

[10] a) S. Fischer, S. Michnick and M. Karplus, *Biochemistry*, 1993, **32**, 13830-13837; b) C. Cox and T. Lectka, *Acc. Chem. Res.*, 2000, **33**, 849-858; c) K. P. Lu, G. Finn, T. H. Lee and L. K. Nicholson, *Nat. Chem. Biol.*, 2007, **3**, 619-629.

[11] G. Fischer, *Chem. Soc. Rev.*, 2000, **29**, 119-127.

[12] a) G. Fischer, *Angew. Chem. Int. Ed.*, 1994, **33**, 1415-1436; b) S. F. Göthel and M. A. Marahiel, *Cell Mol. Life Sci.*, 1999, **55**, 423-436.

[13] Examples of folding kinetics affected by incorporation of fluoroprolines: in β2-microglobulin, a) V. Yu. Torbeev, D. Hilvert, *Proc. Natl. Acad. Sci. USA*, 2013, **110**, 20051-20056; in thioredoxin, b) D. Roderer, R. Glockshuber and M. Rubini, *ChemBioChem*, 2015, **16**, 2162-2166.

[14] a) V. Kubyshkin and N. Budisa, submitted; b) D. Kern, M. Schutkowski and T. Drakenberg, *J. Am. Chem. Soc.*, 1997, **119**, 8403-8408; c) G. Scherer, M. L. Kramer, M. Schutkowski, U. Reimer, G. Fischer, *J. Am. Chem. Soc.*, 1998, **120**, 5568-5574; d) J. Zhang and M. W. German, *Biopolymers*, 2011, **95**, 755-762

[15] N. W. Owens, C. Braun, J. D. O'Neil, K. Marat and F. Schweizer, *J. Am. Chem. Soc.*, 2007, **129**, 11670–11671

[16] V. Kubyshkin, P. Durkin and N. Budisa, *New. J. Chem.*, 2016, **40**, 5209-5220.

[17] M. Shoulders and R. T. Raines, *Annu. Rev. Biochem.*, 2009, **78**, 929-958

[18] S. Busch, C. D. Bruce, C. Redfield, C. D. Lorenz and S. E. McLain, *Angew. Chem. Int. Ed.*, 2013, **52**, 13091-13095.

[19] V. Kubyshkin and N. Budisa, *Org. Biomol. Chem.*, 2017, **15**, 619-627.

[20] a) V. Somayaji and R. S. Brown, *J. Org. Chem.*, 1986, **51**, 2676-2686; b) A. J. Kirby, I. V. Komarov, P. D. Wothers and N. Feeder, *Angew. Chem. Int. Ed.*, 1998, **37**, 785-786; c) A. J. Kirby, I. V. Komarov, and N. Feeder, *J. Am. Chem. Soc.*, 1998, **120**, 7101-7102; d) J. Clayden and W. J. Moran, *Angew. Chem. Int. Ed.*, 2006, **45**, 7118-7120; e) I. V. Komarov, S. Yanik, A. Yu. Ishchenko, J. E. Davies, J. M. Goodman, A. J. Kirby, *J. Am. Chem. Soc.*, 2015, **137**, 926-930; f) R. Szostak, J. Aube and M. Szostak, *J. Org. Chem.*, 2015, **80**, 7905-7927; g) M. Liniger, D. G. VanderVelde, M. K. Takase, M. Shahgholi, B. M. Stolz, *J. Am. Chem. Soc.*, 2016, **138**, 969-974.

[21] The early computation analysis of AcProNHMe suggested that the *syn/exo* and *anti/endo* transition states are most favoured, with the energy difference about 6 kJ mol^{-1}, whereas no saddle point was found for the *syn/endo* state, due to the steric repulsion between the N- and C-terminal groups in this transition state: S. Fischer, R. L. Dunbrack Jr. and M. Karplus, *J. Am. Chem. Soc.*, 1994, **116**, 11931-11937.

[22] S. Adachi, N. Kumagai, M. Shibasaki, *Chem. Sci.*, 2017, **8**, 85-90

[23] See, for example: a) Y. K. Kang and H. Y. Choi, *Biophys. Chem.*, 2004, **111**, 135-142; b) A. E. Aliev, S. Bhandal and D. Courtier-Murias, *J. Phys. Chem. A*, 2009, **113**, 10858-10865; c) J. Chen, S. A. Edwards, F. Gräter and C. Baldauf, *J. Phys. Chem. B*, 2012, **116**, 9346-9351.

[24] E. Vöhringer-Martinez, F. Duarte, A. Toro-Labbé, *J. Phys. Chem. B*, 2012, **116**, 12972-12979.

[25] A. Y. Mercedez-Camacho, A. B. Mullins, M. D. Mason, G. G. Xu, B. J. Mahoney, X. Wang, J. F. Peng and F. A. Etzkorn, *Biochemistry*, 2013, **52**, 7707-7713.

[26] C. Cox, T. Lectka, *J. Am. Chem. Soc.*, 1998, **120**, 10660-10668.

View Article Online
DOI: 10.1039/C7OB01421J

[27] The structures have been deposited in Cabridge Crystallographic Data Centre under the deposition numbers: **2a** – CCDC 1554475, **3a** – CCDC 1554476.
[28] M. Cai, Y. Huang, J. Liu and R. Krishnamoorthi, *J. Biomol. NMR*, 1995, **6**, 123–128.
[29] M. P. Hinderaker and R. T. Raines, *Prot. Sci.*, 2003, **12**, 1188-1194.
[30] C. Siebler, B. Maryasin, M. Kuemin, R. S. Erdmann, C. Rigling, C. Grünenfelder, C. Ochsenfeld and H. Wennemers, *Chem. Sci.*, 2015, **6**, 6725-6730.
[31] C. Renner, S. Alefelder, J. H. Bae, N. Budisa, R. Huber and L. Moroder, *Angew. Chem. Int. Ed.*, 2001, **40**, 923–925.
[32] Somehow higher activation entropy values have been reported for **5a** in E. S. Eberhardt, N. Panasik Jr., R. T. Raines, *J. Am. Chem. Soc.*, 1996, **118**, 12261-12266.
[33] 3-fluoroprolines, a) C. A. Thomas, E. R. Talaty and J. G. Bann, *Chem. Commun.*, 2009, 3366–3368; and 4-trifluroromethylproline, b) V. Kubyshkin, S. Afonin, S. Kara, N. Budisa, P. K. Mykhailiuk and A. S. Ulrich, *Org. Biomol. Chem.*, 2015, **13**, 3171–3181.
[34] 4-fluoroproline, see ref 31; 4-hydroxyproline and its O-glycosylated derivative,s see ref 15, 4-azidoproline see L.-S. Sonntag, PhD Thesis, Basel University, 2005.
[35] a) E. S. Eberhardt, S. N. Loh, A. P. Hinck and R. T. Raines, *J. Am. Chem. Soc.*, 1992, **114**, 5437–5439; b) C. Cox, T. Lectka, *J. Org. Chem.*, 1998, **63**, 2426-2427.
[36] V. S. Kubyshkin, P. K. Mykhailiuk and I. V. Komarov, *Tetrahedron Lett.*, 2007, **48**, 4061-4063.
[37] D. N. Reddy, R. Thirupathi, S. Tumminakatti and E. N. Prabhakaran, *Tetrahedron Lett.*, 2012, **53**, 4413–4417
[38] A. L. Van Geet, *Anal. Chem.*, 1970, **42**, 679–680
[39] V. Frenna, N. Vivona, G. Consiglio and D. Spinelli, *J. Chem. Soc. Perkin Trans. II*, 1985, 1865-1868.
[40] B. Linclau, Z. Wang, G. Compain, V. Paumelle, C. Q. Fontenelle, N. Wells and A. Weymouth-Wilson, *Angew. Chem. Int. Ed.*, 2016, **55**, 674-678.

View Article Online
DOI: 10.1039/C7OB01421J

An experimental model for probing energetics of the amide rotation around proline is described.

View Article Online
DOI: 10.1039/C7OB01421J

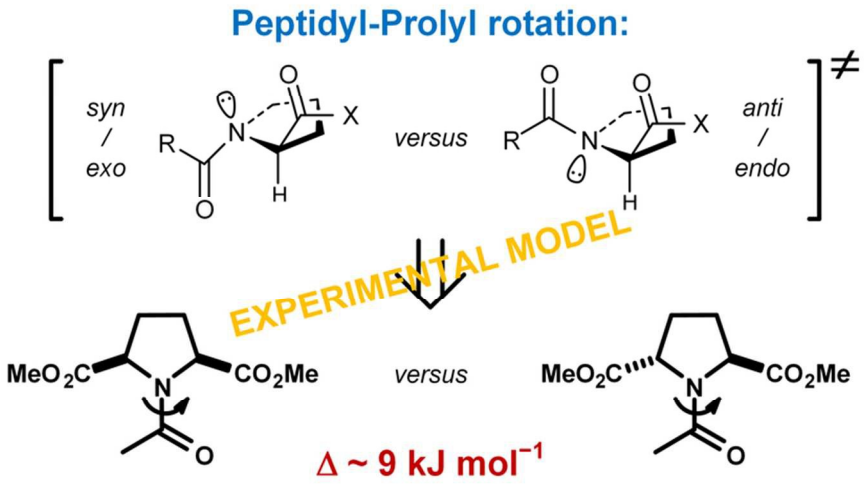

40x20mm (600 x 600 DPI)